

Nonlinear photoluminescence spectra from a quantum-dot-cavity system: Interplay of pump-induced stimulated emission and anharmonic cavity QED

Peijun Yao, P. K. Pathak, E. Illes, and S. Hughes

*Department of Physics, Queen's University Kingston, Ontario, Canada K7L 3N6*S. Münch, S. Reitzenstein, P. Franeck, A. Löffler, T. Heindel, S. Höfling, L. Worschech, and A. Forchel
Technische Physik, Physikalisches Institut, Universität Würzburg and Wilhelm Conrad Röntgen Research Center for Complex Material Systems, Am Hubland, D-97074 Würzburg, Germany

(Received 30 October 2009; published 28 January 2010)

We investigate the power-dependent photoluminescence spectra from a strongly coupled quantum dot-cavity system using a quantum master equation technique that accounts for incoherent pumping, stimulated emission, pure dephasing, and fermion or boson statistics. Analytical spectra at the one-photon correlation level and the numerically exact multiphoton spectra for fermions are presented. Master equation models that neglect stimulated emission processes are shown to lead to unphysical predictions at high powers, such as negative mean photon numbers. We compare to recent experiments on a quantum dot-micropillar cavity system and show that an excellent fit to the data can be obtained by varying only the incoherent pump rates in direct correspondence with the experiments. Our theory and experiments together show convincing evidence for stimulated-emission induced broadening and anharmonic cavity quantum electrodynamics.

DOI: [10.1103/PhysRevB.81.033309](https://doi.org/10.1103/PhysRevB.81.033309)

PACS number(s): 78.67.Hc, 42.50.Pq, 78.55.-m, 78.67.De

Introduction. Single quantum dot (QD) cavity systems facilitate the realization of solid state qubits (quantum bits) and have applications for producing single photons¹⁻³ and entangled photons.^{4,5} Rich in physics and potential applications, the coupled QD cavity has been inspiring theoretical and experimental groups to probe deeper into the underlying physics of both weak and strong coupling regimes of semiconductor cavity quantum electrodynamics (QED). Key signatures of cavity QED include the Purcell effect and *vacuum Rabi oscillations*. Although a well-known phenomenon in atomic cavity optics,⁶ vacuum Rabi splitting in a semiconductor cavity was only realized a few years ago.⁷⁻⁹ Inspired by the recent surge of related experiments, researchers have been working hard to develop new theoretical models to understand the semiconductor cavity QED systems. For example, the persistent excitation of the cavity mode for large exciton-cavity detunings was measured,¹⁰⁻¹² and qualitatively explained by extended theoretical approaches that account for coupling between the *leaky* cavity mode and the exciton, and by showing that the main contribution to the emitted spectrum comes from the cavity-mode emission.¹³⁻¹⁷ These formalisms assume an initially excited exciton or an initially excited leaky cavity mode, and they are valid for low-pump powers. However, an interesting question that has been posed recently for the semiconductor systems, e.g., see Refs. 18–20, is what is the role of an incoherent pump on the photoluminescence (PL) spectra, where the pump can excite the exciton and (or) cavity mode? To experimentally investigate the pump-dependent spectra, two recent experiments have been respectively reported by Münch *et al.*²¹ for a QD-micropillar system, and by Laucht *et al.*²² for a QD-photon crystal system; these measurements clearly show the pump-induced crossover from strong to weak coupling.

In this Brief Report, we present a straightforward master equation (ME) theory that self-consistently includes incoherent pumping, stimulated emission, and pure dephasing. We derive useful analytical results at the level of one-photon correlations and present numerically exact results for the

multiphoton spectra. We reanalyze the Würzburg²¹ experiments directly and show the striking differences with previous models that neglect stimulated emission.^{19,20,22} Accounting for fermion statistics, pure dephasing, and the thermal bath model for the exciton pump, an excellent fit to the data is obtained by only changing the incoherent pump rates in direct correspondence with the experiments.

Cavity System and Model. The system investigated here is shown as a scanning electron microscope (SEM) image in Fig. 1, along with the extended experimental data of Ref. 21. We make the following model assumptions: the cavity is single mode in the frequency of interest; the coupling between the cavity and target QD exciton is described through

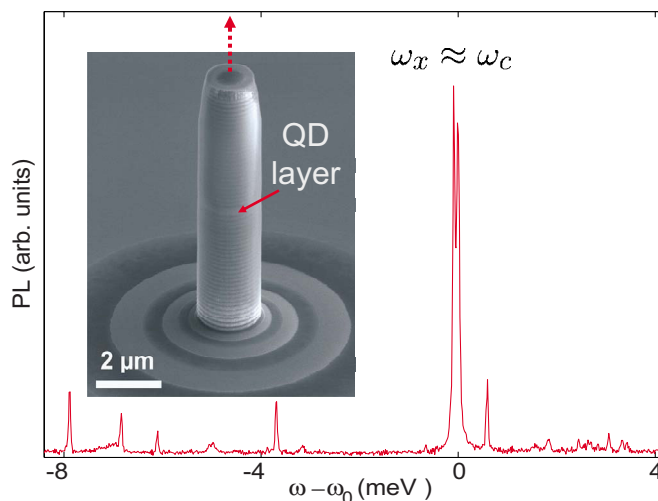


FIG. 1. (Color online) Typical broadband PL spectrum that is emitted when a target exciton is closely resonant with the cavity mode (near $\omega_0=1331.355$ meV); away from the target exciton, there are a series of other exciton levels that can also couple, off-resonantly, to the cavity mode. The SEM image shows our micropillar cavity and the QD layer. The emitted photons from the QDs are detected through vertical emission.

a coupling rate g ; the decay rate of cavity is Γ_c ; for the strongly coupled QD, we include only the target exciton as a system operator, and consider both radiative decay, Γ_x , and pure dephasing, Γ'_x . The QD-cavity system is driven simultaneously by an exciton pump, P_x , and a cavity pump, P_c ; the former is caused by the *incoherent* relaxation of electron-hole pairs from the higher energy level, and the latter is due to the cavity coupling with off-resonant excitons (probably coming from other QDs in the cavity layer). To treat the *incoherent* excitation, we consider a system-reservoir interaction,²³ apply a Born-Markov approximation, and trace over the cavity and target exciton pump reservoirs (*bath approximation*). One has

$$\frac{d\rho}{dt} = \frac{-i}{\hbar}[H_s, \rho] + \mathcal{L}(\rho), \quad (1)$$

with the system Hamiltonian $H_s = \hbar\omega_x \hat{\sigma}^+ \hat{\sigma}^- + \hbar\omega_c \hat{a}^\dagger \hat{a} + \hbar g(\hat{\sigma}^- \hat{a}^\dagger + \hat{\sigma}^+ \hat{a})$, where \hat{a} represents the cavity mode operator, $\hat{\sigma}^{\pm}$ are the Pauli operators of the target QD exciton (with resonance frequency ω_x), and ω_c is the eigenfrequency of the leaky cavity mode. The target exciton and cavity mode get pumped incoherently through the corresponding reservoirs. The density operator of the reservoirs can be written as $\rho_{\text{res}}^O = \sum_k \rho_{kk}^O |n_k^O\rangle \langle n_k^O|$, for $O=x, c$; where ρ_{kk}^O is the density of reservoir modes and n_k^O is the number of photons in the mode of wave vector k . The correlations for the photon reservoir operators \hat{a}_k^c are given by $\langle \hat{a}_k^c \rangle = 0$, $\langle (\hat{a}_k^c)^\dagger \hat{a}_{k'}^c \rangle = \bar{n}_k^c \delta_{kk'}$, and $\langle \hat{a}_k^c (\hat{a}_{k'}^c)^\dagger \rangle = (\bar{n}_k^c + 1) \delta_{kk'}$. Defining the average pump photon number around the cavity frequency as $\bar{n}^c = \bar{n}_k^c$, at $k = \omega_c/c$, yields the effective cavity pump rate: $P_c = \Gamma_c \bar{n}^c$. This incoherent pump process is consistent with the model of Tian and Carmichael.²⁴ The superoperator in Eq. (1) becomes

$$\begin{aligned} \mathcal{L}(\rho) = & \frac{P_c}{2} (2\hat{a}^\dagger \rho \hat{a} - \hat{a} \hat{a}^\dagger \rho - \rho \hat{a} \hat{a}^\dagger), \\ & + \frac{\Gamma_c + P_c}{2} (2\hat{a} \rho \hat{a}^\dagger - \hat{a}^\dagger \hat{a} \rho - \rho \hat{a}^\dagger \hat{a}), \\ & + \frac{P_{12}}{2} (2\hat{\sigma}^+ \rho \hat{\sigma}^- - \hat{\sigma}^- \hat{\sigma}^+ \rho - \rho \hat{\sigma}^- \hat{\sigma}^+) + \frac{P_{21}}{2} (2\hat{\sigma}^- \rho \hat{\sigma}^+ \\ & - \hat{\sigma}^+ \hat{\sigma}^- \rho - \rho \hat{\sigma}^+ \hat{\sigma}^-) + \frac{\Gamma'_x}{4} (\hat{\sigma}_z \rho \hat{\sigma}_z - \rho), \end{aligned} \quad (2)$$

which is in Lindblad form. For the exciton pump we consider two different models, *thermal bath model*, $P_{12} = P_x$ and $P_{21} = \Gamma_x + P_x$; and a *laser model* (heat bath at negative temperatures),²⁵ $P_{12} = P_x$ and $P_{21} = \Gamma_x$; P_x is the target exciton pump rate which is presumed to proportionally follow the experimental pump power, which is an assumption that will be justified later.

One can next derive analytical spectra at the level of one-photon correlations, or compute the exact numerical spectra for n -photon correlations, e.g., see Refs. 20 and 25. We will present both approaches, and begin with the simpler analytical solution. Using Eq. (2), adopting the one-photon-correlation approximation $\langle \hat{\sigma}_z \hat{a} \rangle = -\langle \hat{a} \rangle$, and applying fermion statistics $[\hat{\sigma}^-, \hat{\sigma}^+]_{\pm} = 1$, we exploit the quantum regression theorem²³ to derive the equation of motion for the two-time

correlation functions, $d\langle \hat{a}^\dagger(t) \hat{a}(t+\tau) \rangle / d\tau$ and $d\langle \hat{a}^\dagger(t) \hat{\sigma}^-(t+\tau) \rangle / d\tau$. Subsequently, the steady-state form of the dominant cavity-emitted spectrum¹⁷ is obtained from $S_{\text{cav}}(R, \omega) = F_{\text{cav}}(R) S_{\text{cav}}(\omega)$, with $S_{\text{cav}}(\omega) = \Gamma_c / \pi \lim_{t \rightarrow \infty} \text{Re} \{ \int_0^\infty \langle \hat{a}^\dagger(t) \hat{a}(t+\tau) \rangle e^{i\omega\tau} d\tau \}$, where $F_{\text{cav}}(R)$ is a geometrical factor that depends on the detector/collection optics. We obtain

$$S_{\text{cav}}(\omega) = \frac{\Gamma_c}{\pi} \text{Re} \left[\frac{i \langle \hat{a}^\dagger \hat{a} \rangle_{ss} D(\omega)}{C(\omega) D(\omega) - g^2} + \frac{ig \langle \hat{a}^\dagger \hat{\sigma}^- \rangle_{ss}}{C(\omega) D(\omega) - g^2} \right], \quad (3)$$

where $C(\omega) = \omega - \omega_c + \frac{i}{2} \Gamma_c$ and $D(\omega) = \omega - \omega_x + \frac{i}{2} (P_{21} + P_{12} + \Gamma'_x)$. The subscript “*ss*” represents the steady-state solutions, that are given by

$$\langle \hat{a}^\dagger \hat{a} \rangle_{ss} = \frac{g^2 \Gamma (P_{12} + P_c) + P_c (P_{21} + P_{12}) \left(\frac{\Gamma^2}{4} + \Delta_{cx}^2 \right)}{g^2 \Gamma (P_{21} + P_{12} + \Gamma_c) + \Gamma_c (P_{21} + P_{12}) \left(\frac{\Gamma^2}{4} + \Delta_{cx}^2 \right)}, \quad (4)$$

$$\langle \hat{a}^\dagger \hat{\sigma}^- \rangle_{ss} = \frac{-ig \left(\langle \hat{a}^\dagger \hat{a} \rangle_{ss} - \frac{P_{12}}{P_{21} + P_{12}} \right) \left(i \Delta_{cx} + \frac{\Gamma}{2} \right)}{\frac{\Gamma^2}{4} + \Delta_{cx}^2 + \frac{g^2}{P_{21} + P_{12}} \Gamma}, \quad (5)$$

$$\langle \hat{\sigma}^+ \hat{\sigma}^- \rangle_{ss} = \frac{P_{12} + ig \left(\langle \hat{a}^\dagger \hat{\sigma}^- \rangle_{ss} - \langle \hat{a} \hat{\sigma}^+ \rangle_{ss} \right)}{P_{21} + P_{12}}, \quad (6)$$

where $\Gamma = P_{21} + P_{12} + \Gamma'_x + \Gamma_c$ and $\Delta_{cx} = \omega_c - \omega_x$. To recover boson statistics, one simply replaces the $P_{21} + P_{12}$ terms above by $P_{21} - P_{12}$ and sets Γ'_x to zero. We stress that the above formulas are substantially different to previous models that neglect stimulated emission;^{19,20,22} in particular, we have no unphysical behavior as $\Gamma_c = P_c$, and we get qualitatively different saturation behavior of the QD exciton. Similar incoherent pump models, with pump-induced stimulated emission, have also been recently discussed by Ridolfo *et al.*²⁶

Power Dependent PL. To highlight the underlying physics of pump-induced PL, we proportionally change P_x (and P_c) in our model, and keep all other parameters fixed (i.e., g , Γ_x , and Γ'_x). The fixed parameters are either known for our experimental system, e.g., $\Gamma_x = 0.002$ meV,²⁷ or are accurately obtained from fitting the experimental data at low powers, where $g = 0.045$ meV and $\Gamma_c = 0.08$ meV. We have also included a dominant pure dephasing exciton decay, $\Gamma'_x = 0.035$ meV, likely caused by electron-phonon scattering and spectral diffusion. The chosen values of P_x range from 0.003–1.36 g , and $P_c = 1.6P_x$. The justification for allowing P_c to also follow the power of the laser is due to the fact that our micropillar measurements show a clear linear dependence with power for the cavity mode. For other QD-cavity systems, such as for a few QDs in a photonic crystal cavity, P_c may saturate at much lower powers. In Fig. 2(a), we first show the power-dependent spectra for the thermal bath model (left) and the laser model (right); and in Fig. 2(b), we compare the trend expected from a ME model that neglects stimulated emission processes. The red curves show the one-photon results and the blue curves show the multiphoton case. Although all figures show a similar trend of the doublet becoming a singlet as a function of power, the high-power linewidths are substantially different. In particular, the model with stimulated emission predicts a much larger pump-induced broadening as a function of power. In the absence of stimulated emission, the pump-induced broadening is sup-

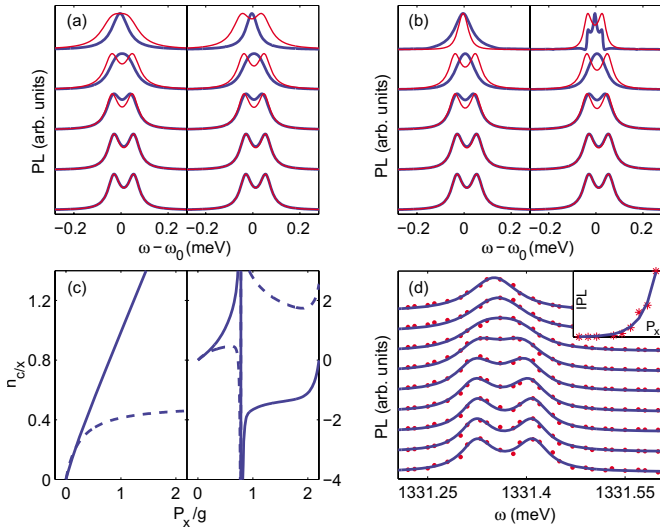


FIG. 2. (Color online) The on-resonance ($\omega_c \approx \omega_x$) PL spectra for different excitation powers. (a) Solution of the ME with two different exciton pump models: thermal bath model (left) and laser model (right). The red (blue) curve is the one photon (multi photon) spectra. The bottom-to-top panels have $P_x = [0.12, 0.5, 4, 16, 64] \cdot 0.02125g(0.0003 - 1.36g)$ and $P_c = 1.6P_x$. (b) ME solution *without* stimulated emission. (c) Mean exciton number (dashed) and photon number (solid), with the thermal-bath model (left); corresponding solution *without* stimulated emission (right). (d) Experimental data corresponding to $P_{\text{exp}} = [0.12, 0.25, 0.5, 2, 4, 8, 16, 32, 64] \mu\text{W}$, and the thermal-bath model fits (multiphoton and stimulated emission included), where $P_{x/c}$ proportionally follows the experimental values; the inset shows the integrated PL (experiment and theory).

pressed, and the larger pump rates result in negative exciton and photon densities. The mean exciton number (dashed) and photon number (solid) are shown in Fig. 2(c) using the multiphoton model. Here, we see the drastic influence on the predicted densities if stimulated emission is not included (right), where negative photon densities are predicted in addition to regimes of $n_x > 1$, both of which are obviously unphysical; though we show the thermal bath case here, the laser model gives similar unphysical results.²⁸ Naturally, with stimulated emission neglected in the model, the regime of $P_c > \Gamma_c$ is phenomenologically not allowed,²⁰ so the top spectra in Fig. 2(b) are not reliable.

The experimental data is shown in Fig. 2(d), alongside the thermal-bath fermion model, and there is a very good correspondence, even when the only fitting parameter is a proportionality constant with P_x . We further remark that even at the one-photon-correlation level, a good fit can also be obtained if one adjusts the proportionality constant; and one of the main points we wish to emphasize here is the importance of including stimulated emission. Although Γ'_x may also be pump-dependent, we find that increasing its value by 1–2 orders of magnitude has little influence on our high-power PL, as the stimulated-emission-induced broadening is by far the dominant source of broadening. To have further confidence in the theoretical interpretation, it is important that the models consistently fit the normalized PL, on and off-resonance, as well as the integrated PL. In this regard, we

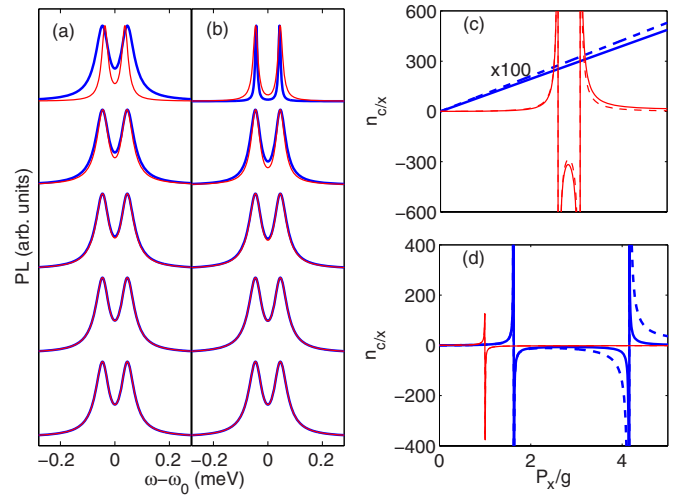


FIG. 3. (Color online) The on-resonance ($\omega_c \approx \omega_x$) PL spectra, for different excitation powers, but for a boson model. (a) ME with stimulated emission, using the thermal bath model (blue) and the laser model for the exciton pump (red). (b) As in (a), but *without* stimulated emission. (c) Corresponding mean density plots: exciton number (dashed) and photon number (solid); for clarity the thermal bath model densities, which are well behaved, are multiplied by 100. (d) As in (c), but *without* stimulated emission.

obtain very good fits to the spectra when the cavity and exciton are off-resonance (not shown) and for the integrated PL [inset in Fig. 2(d)].

Since our QDs are rather large, e.g., elongated with lengths on the order of 100 nm and widths of about 30 nm,⁷ it is natural to present the nonlinear boson PL calculations as well. In Fig. 3, we display the exact boson PL using the two exciton pump models, again with and without stimulated emission terms. Since pure dephasing cannot be included in this boson model, we set the *effective* exciton decay rate $\Gamma_x \rightarrow \Gamma_x + \Gamma'_x$, to have the same overall broadening. Clearly, none of the PL traces follow the trends of the experiments [cf. Fig. 2(d)], and only the thermal bath models produce net positive densities for all pump rates. Moreover, even the low-power PL have different lineshapes due to the important effect of pure dephasing, which acts to suppress the Rabi oscillations without affecting the envelope of the population decay. While it has been discussed before that the boson model²¹ apparently fits well to the same data, since fits were obtained under variation of the coupling constant g and three other free parameters (Γ_x, P_x, P_c), we believe that having so many free parameters (and a model that neglects stimulated emission) can be detrimental to highlighting the correct underlying physics.

High-Pump-Power Inversion and Lasing. Finally, we briefly connect to the prospects for observing one exciton lasing in such a QD-cavity system. It is well known in the field of atomic optics, e.g., see Ref. 25, that the spectral properties of pump-dependent PL can be used to explore the regime of single atom lasing. Characteristic signatures of single state lasing in atomic physics include spectral narrowing, inversion, and a regime of linearly increasing mean photon number as a function of pump power. On the other hand, an incoherent pump of thermal photons will naturally be det-

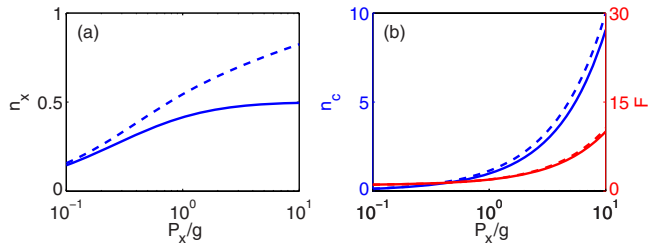


FIG. 4. (Color online) (a) Mean exciton number versus P_x (with $P_c = 1.6P_x$, as before): exciton pump thermal-bath model (solid) and laser model (dashed); both cases include stimulated emission. (b) Corresponding mean photon number (left axis: blue) and Fano factor F (right axis: red).

perimental to the prospect of achieving single photon lasing. In Fig. 4(a) we use two different incoherent exciton pumps, namely, the thermal-bath model (solid) and the laser model (dashed), to investigate the pump-dependent mean exciton number and the mean photon number [panel (b)]. As expected, only the laser model allows inversion, but both models yield a mean photon number of greater than 1. However, the Fano function (photon number variance)²⁹ shows no evidence of a maximum, and thus there is likely no lasing threshold in this system. To achieve single exciton lasing with the present model, we have numerically verified that

one requires a much smaller P_c/P_x ratio and a significantly smaller Γ_c ; for example, $P_c=0$ and $\Gamma_c=0.01$ meV (which is experimentally feasible³⁰) gives a clear lasing threshold and order-of-magnitude reductions in the PL linewidth. Experimental activity on single QD lasers has begun,³¹ and a more detailed multilevel excitation scheme will be needed to connect to these works, which is left to future work.

Conclusions. A ME formalism, with incoherent pumping, pure dephasing, and a QD fermion model, has been introduced and used to investigate the power-dependent PL spectrum of a QD exciton under steady-state pumping. We have shown the importance of self-consistently including stimulated emission, and validated our model by directly comparing with recent experimental data on semiconductor micro-pillar cavities. A very good fit to the data is obtained by *only* changing the pump rates in direct correspondence with the experiments, showing that we are well into the elusive regime of anharmonic semiconductor cavity QED.

This work was supported by the National Sciences and Engineering Research Council of Canada, the Canadian Foundation for Innovation, and the Deutsche Forschungsgemeinschaft via the Research Group *Quantum Optics in Semiconductor Nanostructures* and the State of Bavaria. We thank H. J. Carmichael, J. J. Finley, A. Laucht, and the authors of Ref. 19 for useful comments and suggestions.

¹P. Michler *et al.*, *Science* **290**, 2282 (2000).

²E. Moreau *et al.*, *Appl. Phys. Lett.* **79**, 2865 (2001).

³C. Santori, D. Fattal, J. Vucković, G. S. Solomon, and Y. Yamamoto, *Nature (London)* **419**, 594 (2002).

⁴D. P. J. Ellis, A. J. Bennett, S. J. Dewhurst, C. A. Nicoll, D. A. Ritchie, and A. J. Shields, *New J. Phys.* **10**, 043035 (2008).

⁵See, for example, R. Johne *et al.*, *Phys. Rev. Lett.* **100**, 240404 (2008); P. K. Pathak and S. Hughes, *Phys. Rev. B* **79**, 205416 (2009).

⁶See, e.g., J. McKeever, A. Boca, A. D. Boozer, R. Miller, J. R. Buck, A. Kuzmich, and H. J. Kimble, *Science* **303**, 1992 (2004).

⁷J. P. Reithmaier *et al.*, *Nature (London)* **432**, 197 (2004).

⁸T. Yoshie *et al.*, *Nature (London)* **432**, 200 (2004).

⁹E. Peter, P. Senellart, D. Martrou, A. Lemaître, J. Hours, J. M. Gérard, and J. Bloch, *Phys. Rev. Lett.* **95**, 067401 (2005).

¹⁰K. Hennessy *et al.*, *Nature (London)* **445**, 896 (2007).

¹¹D. Press *et al.*, *Phys. Rev. Lett.* **98**, 117402 (2007).

¹²J. Suffczynski, A. Dousse, K. Gauthron, A. Lemaître, I. Sagnes, L. Lanco, J. Bloch, P. Voisin, and P. Senellart, *Phys. Rev. Lett.* **103**, 027401 (2009).

¹³G. Cui and M. G. Raymer, *Phys. Rev. A* **73**, 053807 (2006).

¹⁴A. Auffeves, B. Besga, J.-M. Gérard, and J.-P. Poizat, *Phys. Rev. A* **77**, 063833 (2008).

¹⁵M. Yamaguchi, T. Asano, and S. Noda, *Opt. Express* **16**, 18067 (2008).

¹⁶A. Naesby, T. Suhr, P. T. Kristensen, and J. Mørk, *Phys. Rev. A* **78**, 045802 (2008).

¹⁷S. Hughes and P. Yao, *Opt. Express* **17**, 3322 (2009).

¹⁸L. V. Keldysh, V. D. Kulakovskii, S. Reitzenstein, M. N. Makhonnin, and A. Forchel, *JETP Lett.* **84**, 494 (2006).

¹⁹F. P. Laussy, E. del Valle, and C. Tejedor, *Phys. Rev. Lett.* **101**, 083601 (2008).

²⁰E. del Valle, F. P. Laussy, and C. Tejedor, *Phys. Rev. B* **79**, 235326 (2009).

²¹S. Münch *et al.*, *Opt. Express* **17**, 12821 (2009).

²²A. Laucht *et al.*, *Phys. Rev. Lett.* **103**, 087405 (2009).

²³H. J. Carmichael, *Statistical Methods in Quantum Optics* (Springer-Verlag, Berlin Heidelberg, 1999).

²⁴L. Tian and H. J. Carmichael, *Quantum Opt.* **4**, 131 (1992).

²⁵M. Löffler, G. M. Meyer, and H. Walther, *Phys. Rev. A* **55**, 3923 (1997).

²⁶A. Ridolfo, O. Di Stefano, S. Portolan, and S. Savasta, arXiv:0906.1455 (unpublished).

²⁷S. Reitzenstein *et al.*, *Phys. Rev. Lett.* **103**, 127401 (2009).

²⁸We do confirm, however, that Ref. 22 has indeed net positive densities, for their chosen parameters.

²⁹The Fano function, $F = (\langle \hat{a}^\dagger \hat{a} - \langle \hat{a}^\dagger \hat{a} \rangle \rangle^2) / \langle \hat{a}^\dagger \hat{a} \rangle$, can be used to assess a lasing threshold, if a clear maximum is obtained, e.g., see Ref. 25.

³⁰S. Reitzenstein *et al.*, *Appl. Phys. Lett.* **90**, 251109 (2007).

³¹Z. G. Xie, S. Götzinger, W. Fang, H. Cao, and G. S. Solomon, *Phys. Rev. Lett.* **98**, 117401 (2007); S. Reitzenstein, C. Böckler, A. Bazhenov, A. Gorbunov, A. Löffler, M. Kamp, V. D. Kulakovskii, and A. Forchel, *Opt. Express* **16**, 4848 (2008); M. Nomura, N. Kumagai, S. Iwamoto, Y. Ota, and Y. Arakawa, *ibid.* **17**, 15975 (2009).